

**Observation of spin glass state in weakly ferromagnetic  $\text{Sr}_2\text{FeCoO}_6$  double perovskite**

Pradheesh R.,<sup>1</sup> Harikrishnan S. Nair,<sup>2</sup> C. M. N. Kumar,<sup>2</sup> Jagat Lamsal,<sup>3</sup> R. Nirmala,<sup>1</sup> P. N. Santhosh,<sup>1</sup> W. B. Yelon,<sup>4</sup> S. K. Malik,<sup>5</sup> V. Sankaranarayanan\*,<sup>1</sup> and K. Sethupathi\*<sup>1</sup>

<sup>1</sup>*Low Temperature Physics Laboratory, Department of Physics,  
Indian Institute of Technology Madras, Chennai 600036,  
India.*

<sup>2</sup>*Jülich Center for Neutron Sciences-2/Peter Grünberg Institute-4,  
Forschungszentrum Jülich, 52425 Jülich, Germany*

<sup>3</sup>*Department of Physics and Astronomy, University of Missouri-Columbia,  
Missouri 65211, USA.*

<sup>4</sup>*Materials Research Center and Department of Chemistry,  
Missouri University of Science and Technology, Rolla, Missouri 65409,  
USA.*

<sup>5</sup>*Departamento de física Teórica e Experimental, Natal-RN, 59072-970,  
Brazil.*

(Dated: 23 November 2011)

We report the observation of spin glass state in the double perovskite oxide  $\text{Sr}_2\text{FeCoO}_6$  prepared through sol-gel technique. Initial structural studies using x rays reveal that the compound crystallizes in tetragonal  $I4/m$  structure with lattice parameters,  $a = 5.4609(2)$  Å and  $c = 7.7113(7)$  Å. The temperature dependent powder x ray studies reveal no structural phase transition in the temperature range 10 – 300 K. However, the unit cell volume shows an anomaly coinciding with the magnetic transition temperature thereby suggesting a close connection between lattice and magnetism. Neutron diffraction studies and subsequent bond valence sums analysis show that in  $\text{Sr}_2\text{FeCoO}_6$ , the  $B$  site is randomly occupied by Fe and Co in the mixed valence states of  $\text{Fe}^{3+}/\text{Fe}^{4+}$  and  $\text{Co}^{3+}/\text{Co}^{4+}$ . The random occupancy and mixed valence sets the stage for inhomogeneous magnetic exchange interactions and in turn, for the spin glass like state in this double perovskite which is observed as an irreversibility in temperature dependent dc magnetization at  $T_f \sim 75$  K. Thermal hysteresis observed in the magnetization profile of  $\text{Sr}_2\text{FeCoO}_6$  is indicative of the mixed magnetic phases present. The dynamic magnetic susceptibility displays characteristic frequency dependence and confirms the spin glass nature of this material. Dynamical scaling analysis of  $\chi'(T)$  yields a critical temperature  $T_{ct} = 75.14(8)$  K and an exponent  $z\nu = 6.2(2)$  typical for spin glasses. The signature of presence of mixed magnetic interactions is obtained from the thermal hysteresis in magnetization of  $\text{Sr}_2\text{FeCoO}_6$ . Combining the neutron and magnetization results of  $\text{Sr}_2\text{FeCoO}_6$ , we deduce the spin states of Fe to be in low spin while that of Co to be in low spin and intermediate spin.

PACS numbers: 75.50.Lk, 75.47.Lx, 75.50.-y

## I. INTRODUCTION

Ferromagnetic double perovskite oxides of general formula  $A_2BB'O_6$  ( $A$  = divalent alkaline earth;  $B$  and  $B'$  = transition metals) have been extensively studied as candidates for magnetoresistive materials.<sup>1,2</sup> The crystallographic ordering of the  $B$  cations in the double perovskites plays an important role in realizing novel magnetic and transport properties including magnetoresistance.<sup>2</sup> Depending on the crystallographic arrangement of  $B$  cations, double perovskites are classified as random, rocksalt or layered.<sup>3</sup> For example, double perovskites like  $\text{Ca}_2\text{FeMoO}_6$  have a rocksalt arrangement<sup>4</sup> while  $\text{PrBaCo}_2\text{O}_{5+\delta}$  adopts a layered structure.<sup>5</sup> Though  $B$  site ordered double perovskites are of interest for magnetoresistive properties and ferromagnetism, it has been observed that comparable ionic radii and oxidation states of different cations at the  $B$  site can lead to mixed crystallographic occupation and result in what is known as antisite disorder.<sup>3</sup> Depending on the type, size and charge of the cations present at the  $B$  site, different magnetic properties varying from antiferromagnetism (AFM)<sup>6,7</sup> to spin glass (SG)<sup>8,9</sup> have been reported for double perovskites. Most of the Fe based double perovskites display a high magnetic transition temperature, which is surprising given the fact that the Fe ions are separated far apart in this compound.<sup>2</sup> However, a few exceptions to this, like  $\text{Sr}_2\text{FeWO}_6$ , have been reported, with a low transition temperatures of  $\approx 37$  K.<sup>10</sup> The correlation between magnetoresistance and magnetism in these compounds and the site disorder is clear from the study comparing the properties of ordered and disordered  $\text{Sr}_2\text{FeMoO}_6$ .<sup>11</sup> The site disorder can partially or completely destroy the  $B$  site ordering of cations and can influence the physical properties like magnitude of magnetization, Curie temperature and low-field magnetoresistance.<sup>12,13</sup> It has been found that the site disorder can be influenced by preparative conditions such as heat treatment temperature<sup>12,14</sup>, treatment time<sup>14</sup> etc., thereby making it possible to tune the magnetic phases of  $A_2BB'O_6$  through a suitable selection of  $B/B'$  cations and preparative conditions. Though double perovskite oxides in the  $A_2BB'O_6$  family have been actively investigated, there are only a few reports on the Co based double perovskite,  $\text{Sr}_2\text{FeCoO}_6$ .<sup>15,16</sup> Earlier studies on the chemically similar single perovskite  $\text{SrFe}_{1-x}\text{Co}_x\text{O}_3$  reported the  $x = 0.5$  composition to be ferromagnetic with a high  $T_c$  of 340 K and saturation magnetic moment of  $3 \mu_B$ .<sup>17,18</sup> Meanwhile, Maignan *et al.*, reported  $\text{SrFe}_{0.5}\text{Co}_{0.5}\text{O}_3$  to be ferromagnetic below  $T_c \sim 200$  K, with a saturation magnetization of  $1.5 \mu_B$  at 5 K, in 1.45 T.<sup>15</sup> *Ab initio* band

structure calculations on the double perovskite  $\text{Sr}_2\text{FeCoO}_6$  showed that Co and Fe make comparable contributions to ferromagnetism.<sup>19</sup> The  $\text{Co}^{4+}(d^5\bar{L})$  and  $\text{Fe}^{4+}(d^4\bar{L})$  in high spin (HS) states can lead to metallicity and ferromagnetism in these systems. However, owing to the comparable ionic radii and valence states of Fe and Co (both in 4+ state), it is surprising that Co doped  $\text{SrFeO}_3$  showed ferromagnetism. The absence of a linear  $B\text{--O--}B'\text{--O--}B$  chain consequent to tilts in the  $BO_6$  and  $B'O_6$  octahedra can cause  $90^\circ$  and  $180^\circ$  superexchange interactions.<sup>20,21</sup> Moreover, the comparable ionic radii of the  $B$  site cations combined with the antisite disorder can lead to magnetic frustration in the double perovskites. Cluster glass phenomenon in  $\text{Sr}_2\text{Mn}_{1-x}\text{Fe}_x\text{MoO}_6$ <sup>20</sup> was attributed to the local magnetic frustration developed due to the competing nearest neighbour ( $NN$ ) and next nearest neighbour ( $NNN$ ) superexchange interactions. Incompatible superexchange interactions and magnetic frustration due to the site disorder of the  $B$  and  $B'$  cations were observed also in  $\text{Sr}_2\text{FeTiO}_{6-\delta}$ .<sup>22</sup> These results point to the fact that mixed valence state of the  $B$  and  $B'$  ions and their crystallographic disorder can lead to a spin glass state as it would create *mixed interactions* and *randomness*.<sup>23</sup> In the present study on  $\text{Sr}_2\text{FeCoO}_6$ , through detailed structural and magnetic investigations, we observe an inhomogeneous magnetic state with the characteristics of a spin glass phase arising from incompatible magnetic interactions and disorder.

## II. EXPERIMENTAL DETAILS

Polycrystalline samples of  $\text{Sr}_2\text{FeCoO}_6$  were prepared following sol-gel method as described elsewhere<sup>24</sup> but, drying the gel at  $120^\circ\text{C}$  and performing the final sintering at  $1050^\circ\text{C}$  for 36 h. X-ray powder diffraction (XRD) patterns were recorded in the temperature range of 10 - 300 K using a Huber diffractometer in Guinier geometry ( $\text{Mo K}_\alpha$ ). Neutron powder diffraction (NPD) measurement at 300 K was performed at the University of Missouri Research Reactor (MURR) with neutron wavelength of  $1.4789 \text{ \AA}$  employing position sensitive detector. The crystal structure was refined by Rietveld method<sup>25</sup> using FULLPROF program.<sup>26</sup> DC and AC magnetic measurements were carried out in a commercial SQUID magnetometer and physical property measurement system (both M/s Quantum Design, USA). DC magnetization in field cooled (FC) and zero-field cooled (ZFC) cycles were performed at different applied fields from 100 to 50 kOe. AC susceptibility was measured using SQUID magnetometer in an ac field of 3 Oe with frequencies of 33, 133, 337, 667, 967, 1333 Hz.

### III. RESULTS AND DISCUSSION

From the powder XRD data, the crystal structure of  $\text{Sr}_2\text{FeCoO}_6$  was refined in the tetragonal space group  $I4/m$  (No. 87) with lattice constants  $a = 5.4568(2)\text{\AA}$  and  $c = 7.7082(4)\text{\AA}$ . A pictorial representation of the  $\text{Sr}_2\text{FeCoO}_6$  double perovskite unit cell is shown in Fig 1. Even though, following the earlier reports on  $\text{SrFe}_{1-x}\text{Co}_x\text{O}_3$ <sup>15</sup> a refinement in cubic  $Pm3m$  space group was undertaken initially, a faithful fit to XRD data was achieved using the tetragonal space group. The results of our Rietveld analysis are presented in Fig 2 (a) where the observed xrd pattern at 300 K, the calculated profile, difference profile and the Bragg peaks are shown. The inset of Fig 2 (a) compares the  $\chi^2$  (goodness-of-fit) of the refinement from  $I4/m$  and  $Pm3m$  and shows that the former gives a better fit. The temperature evolution of unit cell volume is presented in Fig. 2 (b). The variation of cell volume was modelled using the Grüneisen approximation<sup>27</sup>,  $V(T) = \gamma U(T)/K_0 + V_0$ ;  $U(T) = 9 Nk_B T(T/\Theta_D)^3 \int_0^{\Theta_D/T} x^3/(e^x - 1)dx$ . Here,  $\gamma$  is the Grüneisen parameter,  $K_0$  is the incompressibility,  $V_0$  is the volume at  $T = 0$  K and  $\Theta_D$  is the Debye temperature, and the resulting fit is shown as a solid line in Fig. 2 (b). Note that the fit deviates from the data at  $T \sim 75$  K where the volume displays a hump-like feature. This is inferred as magnetoelastic or magnetovolume effect coinciding with the magnetic transition temperature. In this respect, further studies aimed at investigating magneto-structural coupling and polarization measurements would be rewarding. The value of  $\Theta_D$  obtained from the fit is 463(21) K and  $V_0 = 227.89\text{\AA}^3$ . The  $\Theta_D$  of  $\text{Sr}_2\text{FeCoO}_6$  lies in the range of values estimated for similar double perovskites like  $\text{Sr}_2\text{FeTeO}_6$  assuming two different  $\Theta_D$ 's for light and heavy atoms.<sup>28</sup> An important structural parameter characterizing the double perovskites, and having a bearing on the magnetic properties is the cationic site disorder. However, since the x-ray atomic structure factors of Fe and Co are similar, an accurate evaluation of atomic occupancies is not possible from the present XRD data. In order to check the degree of  $B$  site ordering and to confirm the crystal structure of  $\text{Sr}_2\text{FeCoO}_6$  determined by x rays, we performed neutron diffraction experiments (the neutron coherent scattering cross section of Fe and Co are  $11.22 \times 10^{-24}\text{cm}^2$  and  $0.779 \times 10^{-24}\text{cm}^2$  respectively).<sup>29</sup> In Fig 3 we present the neutron diffraction pattern of  $\text{Sr}_2\text{FeCoO}_6$  collected at 300 K along with the results of structure refinement using  $I4/m$  space group. Through Mössbauer studies<sup>30</sup>, it has been confirmed that Fe occupies two distinct crystallographic sites; which supports the choice of  $I4/m$  in our structural analysis.

To confirm the nature of  $B$  site ordering, we carried out the refinement of atomic occupancies using structural models with ordered as well as disordered cationic arrangement at the  $B/B'$  site. A better fit to the experimental data, in terms of profile-match and discrepancy factors was achieved by assuming a disordered model with a random arrangement for the  $B/B'$  cations. The oxygen content was quantified in the refinement process and the deviation from stoichiometry was found to be  $\delta \sim 0.11$ . The structural parameters of  $\text{Sr}_2\text{FeCoO}_6$  including atomic positions, lattice parameters and occupancies and the bond valence sums (BVS) calculated using VaList program<sup>31</sup> are collected in Table I. A rock-salt arrangement of the cations in double perovskites normally occurs if the charge difference between the  $B$  and  $B'$  is greater than 2.<sup>3</sup> In the case of  $\text{Sr}_2\text{FeCoO}_6$ , the charge difference is close to unity as clear from Table I. The BVS calculation from the bond length gives an insight into the oxidation state of the ions and reasonably supports random occupancy at the  $B/B'$  site and mixed valence of Fe and Co. The bond length Fe(2)–O(2) estimated from the structural analysis is 1.969 Å and is comparable to the values found in the literature for double perovskites, especially  $\text{Sr}_2\text{Fe}_{0.75}\text{Cr}_{0.25}\text{MoO}_6$  (Fe–O distance is 1.968 Å).<sup>32</sup> The bond lengths and bond angles obtained from the analysis of NPD data are given in Table II. According to the Glazer's notation, the space group  $I4/m$  has an antiphase tilting along  $c$  axis denoted as  $a^0a^0c^-$  which represents the small shifts of the in-plane oxygen atoms.<sup>33</sup> The magnitude of tilting can be derived from Fe–O–Co ( $\phi$ ) angle as  $(180 - \phi)/2 = 5.65^\circ$ . The average bond length of  $\langle\text{Fe1-O}\rangle$  and  $\langle\text{Fe2-O}\rangle$  are 1.9147 Å and 1.9573 Å, where the latter bond length compare well with the expected value calculated as the sum of the ionic radii of  $\text{Fe}^{3+}$  in low spin state (LS) (0.55 Å) and  $\text{O}^{2-}$  (1.40 Å).<sup>34</sup> Similarly the bond length values for  $\langle\text{Co1-O}\rangle$  (1.9147 Å) and  $\langle\text{Co2-O}\rangle$  (1.9573 Å) are close to the values of the calculated bond length if cobalt has a low spin 4+ valence state ( $r_{LS}=0.518$  Å)<sup>35</sup> and an intermediate spin (IS) 3+ state ( $r_{IS}=0.56$  Å) respectively.<sup>36</sup>

The magnetization profiles of  $\text{Sr}_2\text{FeCoO}_6$  measured at 500 Oe in the zero field-cooled (ZFC) as well as field-cooled cooling (FCC) and warming (FCW) cycles are shown in Fig 4 (a). A magnetic transition is evident at  $T_c \sim 75$  K. The low temperature magnetization data show a marked irreversibility below  $T_c$  indicating the presence of a weak component of ferromagnetism as suggested by Goodenough–Kanamori rules for the  $d^4 - d^5$  cation–anion–cation superexchange<sup>37,38</sup> or spin glass state. With an increase in applied field, the ZFC/FC curves tend to merge and the FC arm shows signs of saturation with broadening of the peak (see

inset (1), Fig 4 (a)). This broadening, also evident in inset (2), Fig 4 (a) where the FC magnetization at higher fields are presented, signifies the presence of majority FM phase since for an antiferromagnet the increase in the field would have had little effect on the sharpness of the transition.<sup>39</sup> The inverse magnetic susceptibility in the temperature range 220 – 350 K was fitted to Curie-Weiss law and the result is presented in Fig 4 (b) where a deviation from the Curie-Weiss (CW) law can be clearly seen for  $T > T_c$ . Deviation from Curie-Weiss behaviour above  $T_c$  attributed to antiferromagnetic spin fluctuations is observed generally in spin glass systems.<sup>40</sup> Previous reports on  $\text{SrFe}_{1-x}\text{Co}_x\text{O}_3$  show that Fe and Co in these solid solutions can possess complex valence states<sup>41</sup> and that, Fe-O-Co superexchange pathways can form which favour electronic transfer from  $\text{Fe}^{3+}$  high spin state (HS,  $S=5/2$ ) to  $\text{Co}^{4+}$  low spin state (LS,  $S=1/2$ ) via superexchange.<sup>15</sup> Complex valence states are observed in the case of  $\text{Sr}_2\text{FeCoO}_6$  from the CW analysis of magnetic susceptibility and is described in detail below. The effective paramagnetic moment calculated from the CW analysis is  $\mu_{eff} = 3.9 \mu_B$ . Keeping in mind that the system is randomly ordered, the effective magnetic moment can be calculated by assuming 50% of Fe and Co (in both  $2a$  and  $2b$  sites) in  $4+$  and  $3+$  spin states. The experimentally obtained effective spin-only moment from the CW fit lies in between the theoretical spin-only moment values of  $\mu_{eff} = 3.67 \mu_B$  and  $\mu_{eff} = 4.12 \mu_B$  (see, Table III). Comparing this with the bond length values obtained we infer that  $\text{Co}^{3+}$  is in intermediate spin state while the valence states of  $\text{Fe}^{3+}$  and  $\text{Fe}^{4+}$  along with  $\text{Co}^{4+}$  are in low spin states. The positive value of Curie-Weiss temperature,  $\Theta_{CW} = 99$  K, calculated from the fit suggests the presence of ferromagnetic interactions in the system. This value is lower than that reported earlier where the role of oxygen non-stoichiometry on ordering temperature was discussed.<sup>41</sup> However, oxygen deficient double perovskites exhibit very low magnetoresistance (MR) which is not the case in  $\text{Sr}_2\text{FeCoO}_6$  since we have observed 68% MR at 12 K at an applied field of 9 T.<sup>30</sup>

Fig 4 (c) shows the plot of FCC and FCW arms measured at 100 Oe where a clear thermal hysteresis below  $T_c$  is discernible. Thermal hysteresis in magnetization cycles are related to the presence of first-order phase transitions with mixed magnetic phases as has been reported in the case of disordered manganites<sup>42,43</sup> or rare earth double perovskite oxides.<sup>44</sup> The end compositions of  $\text{Sr}_2\text{FeCoO}_6 - \text{SrFeO}_3$  and  $\text{SrCoO}_3 -$  possess helical magnetic structure and FM respectively; hence  $\text{Sr}_2\text{FeCoO}_6$  consists of AFM regions where Fe–O–Fe superexchange dominate and FM regions where Co–O–Co which is an ideal scenario for spin glass phase.



Magnetic frustration effects in double perovskite oxides are also reported to show similar thermal hysteresis below  $T_c$  as in the case of  $\text{Sr}_2M\text{ReO}_6$  ( $M = \text{Sc}, \text{Co}$  etc).<sup>45</sup> Drawing parallels, magnetic frustration effects originating from different exchange paths due to multiple valences of Co/Fe can also lead to such effects. We also note that at higher applied fields like 500 Oe (Fig 4 (a)), hysteresis is absent. These features indicate a weak first-order-like phase transition due to the presence of mixed magnetic phases.

The isothermal magnetization curve of  $\text{Sr}_2\text{FeCoO}_6$  at 2 K is shown in the main panel, in Fig 5 (a) while inset (1) presents those at 5, 10 K and , 30 - 300 K (inset 2). Hysteresis is observed below 50 K indicating weak ferromagnetism. With an increase in temperature, a decrease in remanance and coercivity is observed, see Fig 5 (b). As the temperature increases, the irreversibility reduces and becomes sigmoidal at 50 K and above; whereas no saturation is attained even at 50 kOe. A notable feature in the isothermal magnetization curves is the step like behaviour in magnetization at low fields as presented in the enlarged view in Fig 5 (c). Such a behaviour was observed in  $\text{Sr}_2\text{YRuO}_6$  and has been attributed to spin flop transition taking place at a critical field.<sup>39</sup> However, the aptness of such an explanation in the case of  $\text{Sr}_2\text{FeCoO}_6$  cannot be tested until the magnetic structure is ascertained.

Sharpness of the peak in ac susceptibility curves and its shift to high temperature with increasing frequency are typical features exhibited by SG systems.<sup>23,46</sup> In order to probe this, ac susceptibility measurements were performed in the temperature range 5 – 90 K, with a driving field of 3 Oe. Fig 6 (a) shows the temperature dependence of the real part of ac susceptibility,  $\chi'(T)$ , at different applied frequencies in the range 33 - 1333 Hz.  $\chi'(T)$  attains a maximum at  $T_f$ , the freezing temperature, that shifts to higher temperature as the frequency is increased. This behaviour is characteristic of SG<sup>23</sup> and is clear from Fig 6 (b). A fit to the Arrhenius relation,  $\omega = \omega_0 \exp[E_a/k_B T]$ , where  $E_a$  is the activation energy, yielded unphysical values of  $\omega_0 = 10^{82}$  Hz and  $E_a = 14301$  eV. The failure of Arrhenius relation points to SG behaviour, since a description of mere energy-barrier blocking and thermal activation will not suit the SG transition. To confirm the spin glass behaviour, analysis of the dynamical scaling at  $T_c$  was performed. For a spin glass, the critical relaxation time  $\tau$  should follow a power law divergence of the form,  $\tau = \tau_0 \left( \frac{T_f}{T_{ct} - T_f} \right)^{z\nu}$  where  $T_{ct}$  is the critical temperature and  $z\nu$  and  $\tau_0$  are the critical exponents and microscopic time scale respectively.<sup>23</sup> The best fit to the above equation, as shown in Fig 6 (c) (inset presents the same graph in log-log scales), yields  $z\nu = 6.2(2)$ ,  $T_{ct} = 75.14(8)$  K and  $\tau_0 \approx 10^{-12}$ s.



The values of  $\tau_0$  and  $z\nu$  are consistent with that of the conventional 3D spin glasses<sup>47</sup> and Fe doped cobaltites.<sup>48</sup> In order to probe whether the FM state coexist with the frozen spin glass state as in *reentrant* spin glasses, we performed ac susceptibility measurements with superimposed dc fields. The result is presented in Fig 6 (d) which shows the out of phase susceptibility in an external dc field varying from 50 - 1000 Oe at a frequency of 33 Hz with an ac amplitude of 3 Oe. We do not observe emergence of a second peak as observed in certain *reentrant* systems<sup>49</sup>, instead, the intensity of the peak at  $T_c$  in  $\chi''(T)$  diminishes with increasing field indicating FM nature of the sample. The ac susceptibility studies confirm the presence of canonical SG state in  $\text{Sr}_2\text{FeCoO}_6$  in turn suggests the presence of disorder; since disorder is a key ingredient for SG behaviour.

To summarize the results, we find that  $\text{Sr}_2\text{FeCoO}_6$  crystallizes in tetragonal  $I4/m$  where the  $B$  site is randomly occupied by Fe and Co in  $2a$  and  $2b$  sites, a finding also supported by the bond valence sums. The Fe and Co cations exist in mixed valence states of  $+3$  and  $+4$  in  $\text{Sr}_2\text{FeCoO}_6$ . The random crystallographic occupation and mixed valency sets the stage for mixed FM and AFM interactions between the transition metal cations and in turn, lead to inhomogeneous magnetism. In a perfectly ordered double perovskite, the magnetic exchange is predominantly governed by the ferromagnetic  $\text{Fe}^{3+}\text{--O}^{2-}\text{--Co}^{4+}$ . With the occurrence of site disorder, additional exchange paths are introduced for example, Fe–Fe or Co–Co which are antiferromagnetic. The spin glass phase with a  $T_c \sim 75$  K that appears in  $\text{Sr}_2\text{FeCoO}_6$  has its origin in the multiple exchange paths that arise due to the mixed interactions. The magnetic moment at 5 K ( $0.39\mu_B$ ) suggests that the transition metal ions in this compound are in a mixed valence state unlike a high-spin tetravalent state as in  $\text{SrFe}_{0.5}\text{Co}_{0.5}\text{O}_3$ .<sup>50</sup> The magnetic ordering of double perovskites is a function of the strength of the  $NN$  and  $NNN$  interactions<sup>51</sup> and the competition between these interactions is known to lead to magnetic frustration effects in  $\text{Ln}_2\text{LiRuO}_6$  ( $\text{Ln} = \text{Pr}, \text{Nd}, \text{Eu}, \text{Gd}, \text{Tb}$ )<sup>52</sup> and  $\text{LaBaCoNbO}_6$ .<sup>53</sup> Depending on the strength of  $NN$  and  $NNN$  interactions materials are classified as Type *I* (strength of AFM interaction is negligible), Type *II* (dominant  $NNN$  interaction) and Type *III* (strength of AFM interaction significant but less than  $NN$  interaction). Type *II* antiferromagnetic structure leads to disorder and yields a ferromagnetic  $NN$  interaction along with an antiferromagnetic  $NNN$  interaction.<sup>28</sup> The presence of disorder leading to spin glass behaviour in  $\text{Sr}_2\text{FeCoO}_6$  shows that the  $NNN$  interaction is not negligible in double perovskite systems. SG behaviour due to incompatible superexchange interactions and mag-

netic frustration was shown by the double perovskites,  $\text{Sr}_2\text{FeTiO}_6$ <sup>22</sup> and  $\text{Sr}_2\text{FeTaO}_6$ .<sup>6</sup> Since  $\text{Fe}^{3+}$  and  $\text{Co}^{4+}$  are isoelectronic, they interact ferromagnetically through the  $NN$  Fe–O–Co superexchange interaction. However, presence of like-pairs of Fe and Co leads to Fe–O–Co–O–Fe  $NNN$  antiferromagnetic superexchange interaction also.<sup>21</sup> The competition between the  $NN$  and  $NNN$  interactions is the origin of the magnetic frustration in  $\text{Sr}_2\text{FeCoO}_6$  which results in a spin glass state. One of the structural aspect affecting the strength of the nearest neighbour interaction is B–O–B' angle. The  $NN$  interaction is stronger if the Fe–O–Co bond angle is near to or equal to  $180^\circ$  in which case, a ferromagnetic interaction manifests. A deviation from the linear Fe–O–Co chain in the case of  $\text{Sr}_2\text{FeCoO}_6$  was clear from the powder neutron diffraction analysis where a bond angle equal to  $168.98^\circ$  was estimated which in turn indicates weak  $NN$  interaction. The weak  $NN$  interaction also explains the observation of a lower  $T_c$  and the low magnetic moment for  $\text{Sr}_2\text{FeCoO}_6$ .

#### IV. CONCLUSIONS

$\text{Sr}_2\text{FeCoO}_6$  synthesized using sol-gel method crystallizes in tetragonal  $I4/m$  structure with disordered cation occupancy. Using neutron diffraction studies, we have confirmed the crystal structure and the subsequent bond valence sums confirm mixed valence for Fe and Co. The different valences of Fe and Co and their mixed occupation in the lattice leads to competition between  $NN$  and  $NNN$  exchange interactions which is also supported by the bond angles estimated. DC magnetization measurements show irreversibility at  $\sim 75$  K where the spin glass phase sets in. The weak component of ferromagnetism observed in magnetization can be due to the competing antiferromagnetic and ferromagnetic interactions and is clear from the low values of remnance. The spin glass state in  $\text{Sr}_2\text{FeCoO}_6$  is further supported by the frequency dependence of real component of ac susceptibility. Dynamical scaling analysis confirms the spin glass phase with  $T_{ct} = 75.14(8)$  K. We propose that spin glass behaviour is due to the magnetic frustration resulting from the competing  $NN$  and  $NNN$  interactions which originate from mixed occupation of cations sites. Our work emphasize that the cationic disorder leads to a spin glass state. The structural and magnetic studies also lead to the deduction of the spin states of Fe and Co in  $\text{Sr}_2\text{FeCoO}_6$ .

## ACKNOWLEDGEMENTS

The authors acknowledge the Department of Science and Technology (DST), India for the financial support for providing the facilities used in this study (Grant No. SR/FST/PSII-002/2007) and (Grant No. SR/NM/NAT-02/2005). PR wishes to thank M. Angst and K. Balamurugan for fruitful discussions.

\* vsn@physics.iitm.ac.in, ksethu@physics.iitm.ac.in

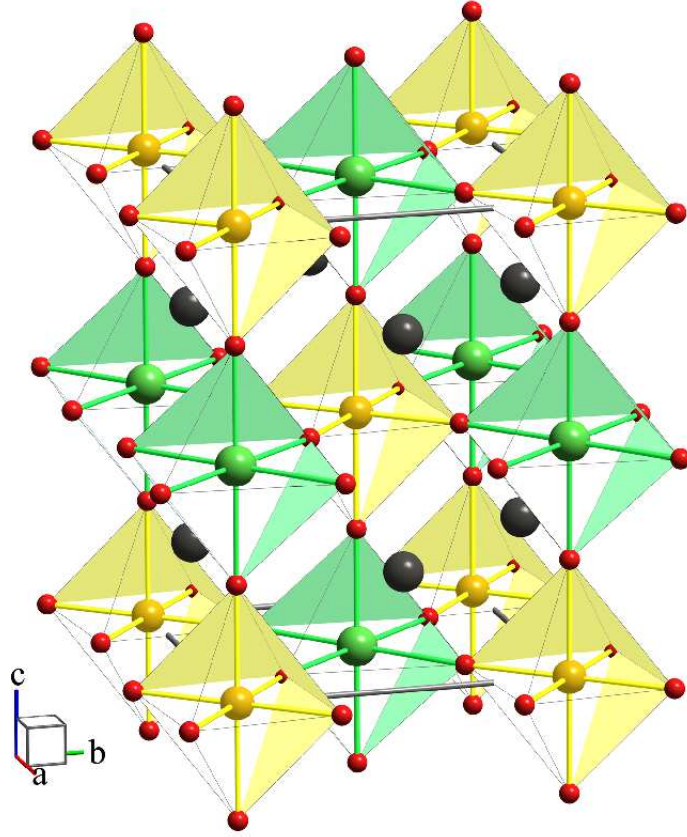


FIG. 1. The tetragonal structure of the double perovskite  $\text{Sr}_2\text{FeCoO}_6$ . The oxygen atoms are represented by red spheres while Co are green, Fe are yellow and Sr are dark grey. The  $\text{CoO}_6$  and  $\text{FeO}_6$  octahedra are also indicated. For succinctness the structure shown is of the  $B$  site ordered type.

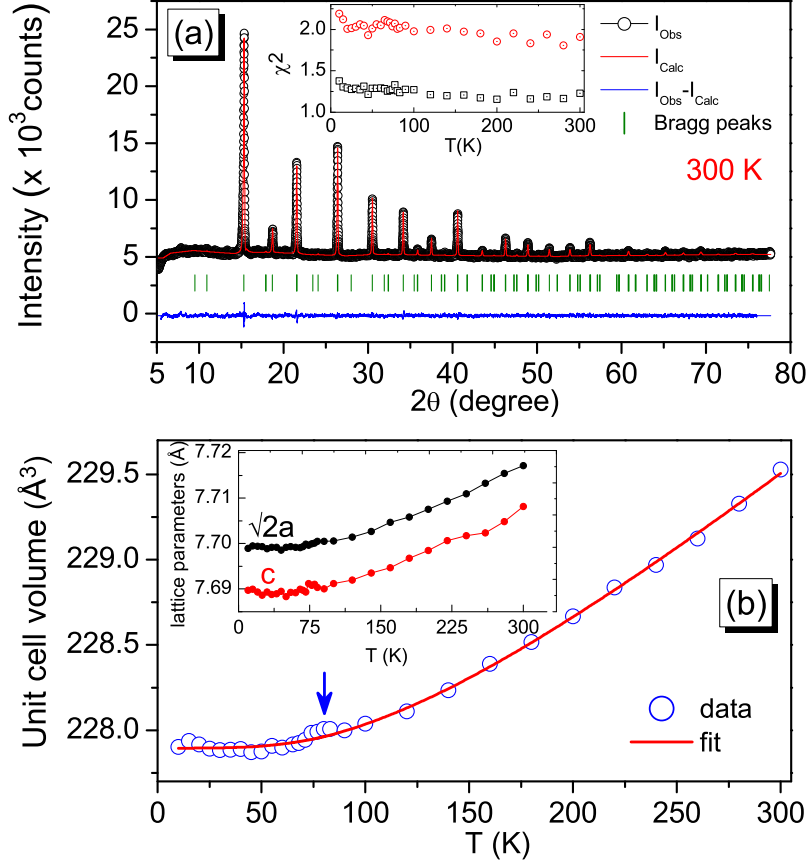


FIG. 2. (a) X-ray diffraction pattern of  $\text{Sr}_2\text{FeCoO}_6$  at 300 K refined in tetragonal  $I4/m$  space group. Quality measures of refinement are  $R_{wP} = 1.52\%$ ,  $R_P = 1.18\%$ ,  $\chi^2 = 1.23$ . (b) Shows the analysis of unit cell volume using Grüneisen approximation. Note the anomaly in volume indicated by arrow. The inset shows temperature evolution of lattice parameters  $\sqrt{2}a$  and  $c$  (the error bars were smaller than the size of the data markers).

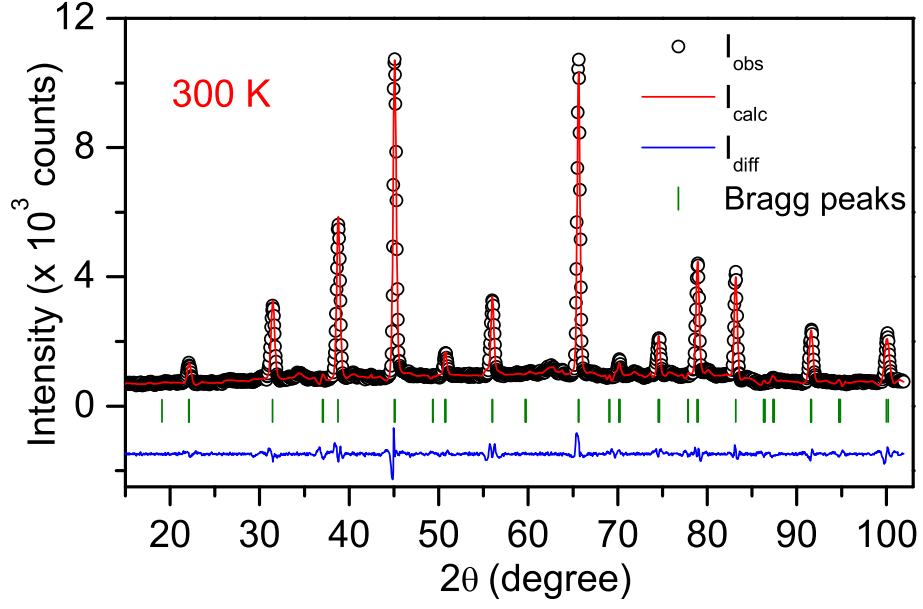


FIG. 3. (a) Observed ( $I_{obs}$ ), calculated ( $I_{calc}$ ) and difference ( $I_{diff}$ ) profiles of neutron diffraction pattern of  $\text{Sr}_2\text{FeCoO}_6$  at 300 K refined in tetragonal  $I4/m$  space group. Vertical markers correspond to Bragg peaks. Quality measures of refinement are  $R_{wP} = 17.6\%$ ,  $R_P = 14.6\%$ ,  $\chi^2 = 3.38$ .

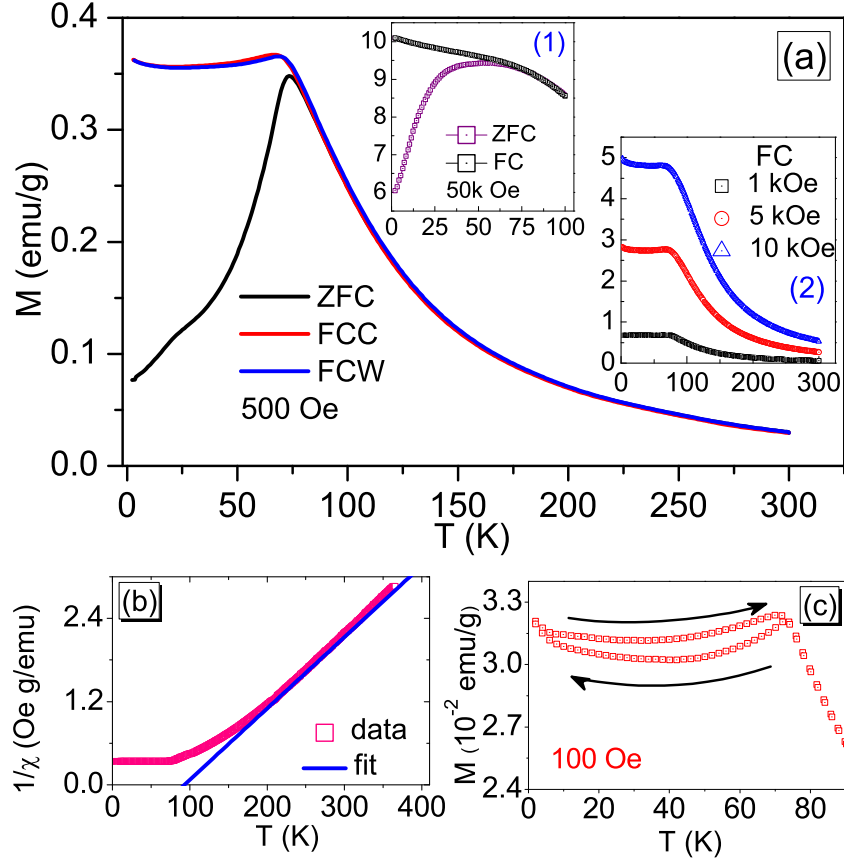


FIG. 4. (a) ZFC and FC (cooling/warming) cycles of magnetization of  $\text{Sr}_2\text{FeCoO}_6$  as a function of temperature at 500 Oe. Inset (1) shows the ZFC/FC curves at 50 kOe and (2) FC curves at different applied fields. (b) Temperature dependence of inverse magnetic susceptibility along with Curie-Weiss fit. (c) Thermal hysteresis observed in FC arm at 100 Oe.



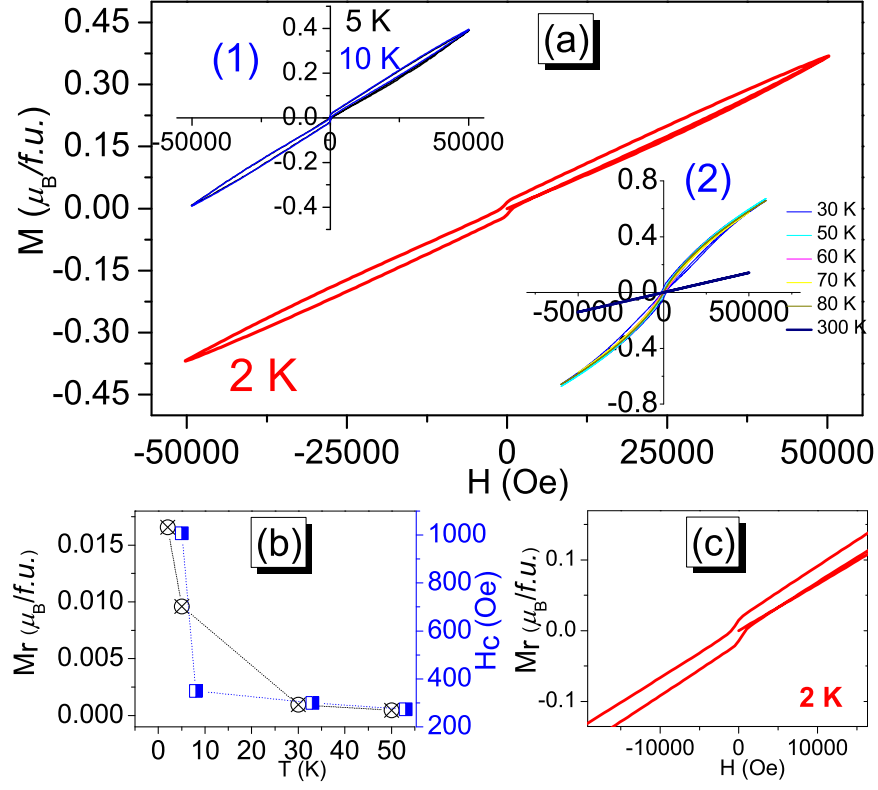


FIG. 5. (a) Isothermal magnetization of  $\text{Sr}_2\text{FeCoO}_6$  at 2 K. Insets (1) and (2) present isotherms at elevated temperatures. (b) Variation of remnant magnetization,  $M_r$  and coercive field,  $H_c$  with temperature. (c) An enlarged view of the magnetization isotherms at 2 K for low fields.

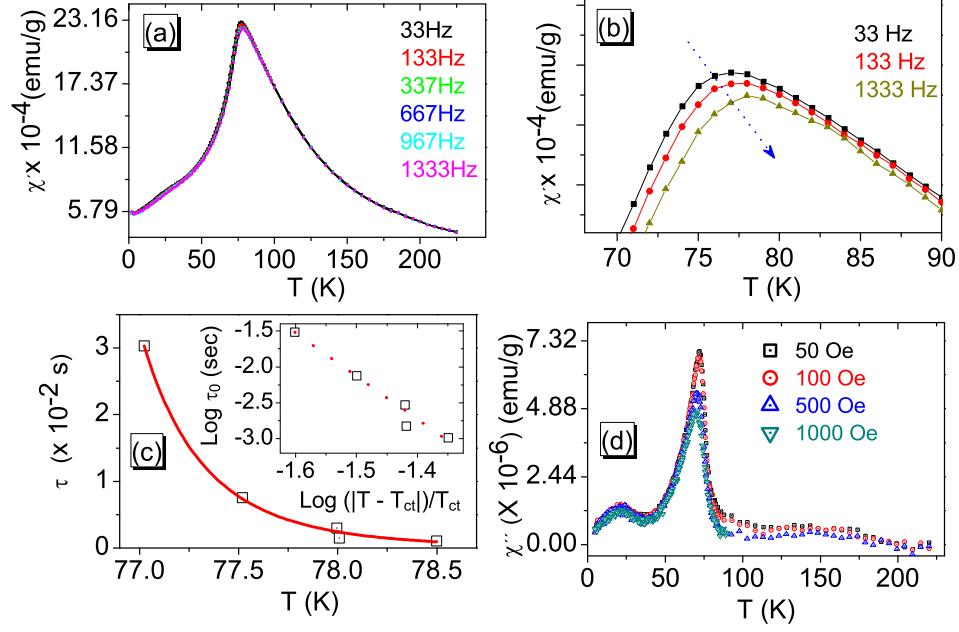


FIG. 6. (a) Temperature dependence of AC susceptibility of  $\text{Sr}_2\text{FeCoO}_6$  at different frequencies. (b) The peak in  $\chi'(T) \sim 75$  K which shifts to higher temperature as the frequency is increased, signifying glassy magnetism. (c) The fit using the power law for critical slowing down, where the best fit gave  $z\nu = 6.2$ ,  $\tau_0 = 10^{-12}$  s. The inset presents the same plot but in log-log scale. (d) Displays  $\chi''(T)$  at different values of superimposed magnetic fields.

TABLE I. Occupancy and bond valence sums (BVS) and (x,y,z) values obtained after Rietveld refinement of the neutron data at 300 K. The unit cell parameters are  $a = 5.4609(2)\text{\AA}$ ,  $b = 5.4609(2)\text{\AA}$  and  $c = 7.7113(7)\text{\AA}$ . The quality of the fit is indicated by the discrepancy factors,  $R_{WP} = 17.6\%$ ,  $R_P = 14.6\%$  and the goodness-of-fit,  $\chi^2 = 3.38$ .

Atom	Site	x	y	z	Occupancy	BVS
Sr	$4d$	0	0.5	0.25	0.25	2.336(9)
Fe1/Co1	$2a$	0	0	0	0.0625	4.055(69)/3.650(62)
Fe2/Co2	$2b$	0	0	0.5	0.0625	3.51(41)/2.967(54)
O1	$4e$	0	0	0.24739(3)	0.25994(10)	1.970(38)
O2	$8h$	0.26798(13)	0.21981(18)	0	0.47621(6)	1.985(15)

TABLE II. Selected bond angles and bond lengths of  $\text{Sr}_2\text{FeCoO}_6$  obtained from the structural analysis.

Bond length ( $\text{\AA}$ )	Bond angle (deg)
Fe1/Co1-O1	$1.9227(15) \times 2$
Fe1/Co1-O2	$1.9107(15) \times 4$
Fe2/Co2-O1	$1.9329(15) \times 2$
Fe2/Co2-O2	$1.9695(15) \times 4$
Fe1-O2-Co2	$168.6988(5)$

TABLE III. Calculated spin only moments ( $\mu_{SO}^2 = \mu_{2a}^2 + \mu_{2b}^2$ ) for  $\text{Sr}_2\text{FeCoO}_6$  assuming the possible spin state values. The calculated spin only moment ( $\mu_{eff.}$ ) lies in between the last two configurations. Note that  $\text{Co}^{3+}$  HS  $S = 2$ , LS  $S = 0$ , IS  $S = 1$  ;  $\text{Co}^{4+}$  HS  $S = 5/2$ , LS  $S = 1/2$  ;  $\text{Fe}^{3+}$  HS  $S = 5/2$ , LS  $S = 1/2$  ;  $\text{Fe}^{4+}$  HS  $S = 2$ , LS  $S = 1$ .

2a	2b	$\mu_{SO}(\mu_B)$
$\text{Co}^{4+}_{HS}(S = 5/2); \text{Fe}^{4+}_{HS}(S = 2)$	$\text{Co}^{4+}_{HS}(S = 5/2); \text{Fe}^{4+}_{HS}(S = 2)$	7.68
$\text{Co}^{3+}_{HS}(S = 2) ; \text{Fe}^{4+}_{HS}(S = 2)$	$\text{Co}^{4+}_{HS}(S = 5/2); \text{Fe}^{4+}_{HS}(S = 5/2)$	7.68
$\text{Co}^{4+}_{HS}(S = 5/2); \text{Fe}^{4+}_{LS}(S = 1)$	$\text{Co}^{4+}_{HS}(S = 5/2); \text{Fe}^{4+}_{LS}(S = 1)$	6.56
$\text{Co}^{4+}_{LS}(S = 1/2); \text{Fe}^{4+}_{HS}(S = 2)$	$\text{Co}^{4+}_{LS}(S = 1/2); \text{Fe}^{4+}_{HS}(S = 2)$	5.19
$\text{Co}^{4+}_{LS}(S = 1/2); \text{Fe}^{4+}_{LS}(S = 1)$	$\text{Co}^{4+}_{LS}(S = 1/2); \text{Fe}^{4+}_{LS}(S = 1)$	3.32
$\text{Co}^{4+}_{LS}(S = 1/2); \text{Fe}^{4+}_{LS}(S = 1)$	$\text{Co}^{3+}_{IS}(S = 1) ; \text{Fe}^{4+}_{LS}(S = 1)$	3.67
$\text{Co}^{3+}_{IS}(S = 1) ; \text{Fe}^{4+}_{LS}(S = 1)$	$\text{Co}^{4+}_{IS}(S = 3/2); \text{Fe}^{3+}_{LS}(S = 1/2)$	4.12

## REFERENCES

- <sup>1</sup>D. Serrate, J. M. De Teresa, M. R. Ibarra, J. Phys.: Condens. Matter **19**, 023201 (2007).
- <sup>2</sup>D. D. Sarma, E. V. Sampathkumaran, S. Ray, R. Nagarajan, S. Majumdar, A. Kumar, G. Nalini, and T. N. Guru Row, Solid State Comm. **114**, 465 (2000).
- <sup>3</sup>M. T. Anderson, K. B. Greenwood, G. A. Taylor, and K. R. Poeppelmeier, Prog. Solid State Chem. **22**, 197 (1993).
- <sup>4</sup>J. Gopalakrishnan, A. Chattopadhyay, S. B. Ogale, T. Venkatesan, R. L. Greene, A. J. Mills, K. Ramesha, B. Hannoyer, and G. Marest, Phys. Rev. B **62**, 9538 (2000).
- <sup>5</sup>S. Streule, A. Podlesnyak, J. Mesot, M. Medarde, K. Conder, E. Pomjakushina, E. Mitberg, and V. Kozhevnikov, J. Phys.: Condens. Matter **17**, 3317 (2005).
- <sup>6</sup>E. J. Cussen, J. F. Vente, P. D. Battle, and T. C. Gibb, J. Mater. Chem. **7**, 459 (1997).
- <sup>7</sup>K. I. Kobayashi, T. Okuda, Y. Tomioka, T. Kimura, and Y. Tokura, J. Magn. Magn. Mater. **218**, 17 (2000).
- <sup>8</sup>P. D. Battle, T. C. Gibb, C. W. Jones, and F. Studer, J. Solid State Chem. **78**, 281 (1989).
- <sup>9</sup>A. Poddar, R. N. Bhowmik, I. P. Muthuselvam, and N. Das, J. Appl. Phys. **106**, 073908 (2009).
- <sup>10</sup>H. Kawanaka, I. Hase, S. Toyama, and Y. Nishihara, Physica B **281**, 518 (2000).
- <sup>11</sup>J. Navarro, Ll. Balcells, F. Sandiumenge, M. Bibes, A. Roig, B. Martínez, J. Fontcuberta, J. Phys.: Condens. Matter **13**, 8481 (2001).
- <sup>12</sup>Ll. Balcells, J. Navarro, M. Bibes, A. Roig, B. Martínez, and J. Fontcuberta, Appl. Phys. Lett. **78**, 781 (2001).
- <sup>13</sup>M. García-Hernández, J. Martínez, M. J. Martínez-Lope, M. T. Casais, and J. A. Alonso, Phys. Rev. Lett. **86**, 2443 (2001).
- <sup>14</sup>H. Sakuma, T. Taniyama, Y. Kitamoto, and Y. Yamazaki, J. Appl. Phys. **93**, 2816 (2003).
- <sup>15</sup>A. Maignan, C. Martin, N. Nguyen, and B. Raveau, Solid State Sci. **3**, 57 (2001).
- <sup>16</sup>P. Bezdzicka, L. Fournés, A. Wattiaux, J. C. Grenier, and M. Pouchard, Solid State Comm. **91**, 501 (1994).
- <sup>17</sup>T. Takeda and H. Watanabe, J. Phys. Soc. Jpn **33**, 973 (1972).
- <sup>18</sup>S. Kawasaki, M. Takano, and Y. Takeda, J. Solid State Chem. **121**, 174 (1996).
- <sup>19</sup>V. V. Bannikov, I. R. Shein, V. L. Kozhevnikov, and A. L. Ivanovskii, J. Struc. Chem. **49**, 781 (2008).

- <sup>20</sup>A. Poddar, and C. Mazumdar, J. Appl. Phys. **106**, 093908 (2009).
- <sup>21</sup>N. C. El'ad, J. D. Jorgensen, M. V. Lobanov, and M. Greenblatt, Phys. Rev. B **67**, 134431 (2003).
- <sup>22</sup>T. C. Gibb, P. D. Battle, S. K. Bollen, and R. J. Whitehead, J. Mater. Chem. **2**, 111 (1992).
- <sup>23</sup>J. A. Mydosh, *Spin Glasses: An experimental Introduction* London: Taylor and Francis, 1993.
- <sup>24</sup>I. G. Deac, S. V. Diaz, B. G. Kim, S. W. Cheong, and P. Schiffer Phys. Rev. B **65**, 174426 (2002).
- <sup>25</sup>H. M. Rietveld, J. Appl. Cryst. **2**, 65 (1969).
- <sup>26</sup>J. Rodriguez-Carvajal, Physica B **192**, 55 (1993).
- <sup>27</sup>D. C. Wallace, *Thermodynamics of crystals* Dover, New York, (1998).
- <sup>28</sup>L. Ortega-San Martin, J. P. Chapman, L. Lezama, J. J. S. Garitaonandia, J. S. Marcos, J. Rodríguez-Fernández, M. I. Arriortua, and T. Rojo, J. Mater. Chem. **16**, 66 (2006).
- <sup>29</sup>*Data from neutron news* **3**, 29 (1992), URL <http://www.ncnr.nist.gov/resources/n-lengths>.
- <sup>30</sup>Pradheesh R., Harikrishnan S. Nair, A. T. Satya, A. Bharathi, R. Nirmala, K. Sethupathi, and V. Sankaranarayanan, in preparation (2011).
- <sup>31</sup>A. S. Wills, A. D. Brown, VaList, CEA, France.
- <sup>32</sup>J. Blasco, C. Ritter, L. Morellon, P. A. Algarabel, J. M. De Teresa, D. Serrate, J. García, and M. R. Ibarra, Solid State Sci., **4**, 651 (2002).
- <sup>33</sup>A. M. Glazer, Acta Crystallogr. Sect. A, **28**, 3384 (1972).
- <sup>34</sup>R. D. Shannon, Acta Crystallogr. Sect. A, **32**, 751 (1976).
- <sup>35</sup>H. Taguchi, M. Shimada, and M. Koizumi, J. Solid State Chem., **29**, 221 (1979).
- <sup>36</sup>P. G. Radaelli and S. W. Cheong, Phys. Rev. B, **66**, 094408 (2002).
- <sup>37</sup>J. B Goodenough, Phys. Rev. **100**, 564 (1955).
- <sup>38</sup>J. Kanamori, J. Phys. Chem. Solids **10**, 87 (1959).
- <sup>39</sup>G. Cao, Y. Xin, C. S. Alexander, and J. E. Crow, Phys. Rev. B **63**, 184432 (2001).
- <sup>40</sup>K. V. Rao, M. Föhnle, E. Figueroa, O. Beckman, and L. Hedman, Phys. Rev. B, **27**, 3104 (1983).
- <sup>41</sup>A. Muñoz, J. Alonso, M. Martínez-Lope, C. de La Calle, and M. Fernández-Díaz, J. Solid State Chem. **179**, 3365 (2006).



- <sup>42</sup>A. A. Wagh, P. S. Anil Kumar, H. L. Bhat, and S. Elizabeth, J. Phys.: Condens. Matter **22**, 026005 (2010).
- <sup>43</sup>J. W. Lynn, R. W. Erwin, J. A. Borchers, Q. Huang, A. Santoro, J. L. Peng, and Z. Y. Li, Phys. Rev. Lett. **76**, 4046 (1996).
- <sup>44</sup>R. I. Dass and J. B. Goodenough, Phys. Rev. B **67**, 14401 (2003).
- <sup>45</sup>H. Kato, T. Okuda, Y. Okimoto, Y. Tomioka, K. Oikawa, T. Kamiyama, and Y. Tokura, Phys. Rev. B **69**, 184412 (2004).
- <sup>46</sup>J. L. Tholence, Solid State Comm. **88**, 917 (1993).
- <sup>47</sup>K. Gunnarsson, P. Svedlindh, P. Nordblad, L. Lundgren, H. Aruga, and A. Ito, Phys. Rev. Lett. **61**, 754 (1988).
- <sup>48</sup>X. Luo, W. Xing, Z. Li, G. Wu, and X. Chen, Phys. Rev. B **75**, 054413 (2007).
- <sup>49</sup>M. Viswanathan and P. S. Anil Kumar, Phys. Rev. B **80**, 012410 (2009).
- <sup>50</sup>M. Abbate, G. Zampieri, J. Okamoto, A. Fujimori, S. Kawasaki, and M. Takano, Phys. Rev. B **65**, 165120 (2002).
- <sup>51</sup>P. D. Battle, and W. J. Macklin, J. Solid State Chem. **52**, 138 (1984).
- <sup>52</sup>S. J. Makowski, J. A. Rodgers, P. F. Henry, J. P. Attfield, and J. W. G. Bos, Chem. Mater. **21**, 264 (2008).
- <sup>53</sup>J. W. Bos, and J. P. Attfield, Phys. Rev. B **70**, 174434 (2004).